CDDpress

www.nature.com/cddiscovery

ARTICLE OPEN

Transient receptor potential ankyrin 1 (TRPA1) mediates reactive oxygen species-induced Ca^{2+} entry, mitochondrial dysfunction, and caspase-3/7 activation in primary cultures of metastatic colorectal carcinoma cells

Pawan Faris[1], Agnese Rumolo[2], Giorgia Pellavio[3], Matteo Tanzi[2], Mauro Vismara[1], Roberto Berra-Romani[4], Andrea Gerbino[5], Salvatore Corallo[6], Paolo Pedrazzoli[6], Umberto Laforenza[3], Daniela Montagna[2,7,8]✉ and Francesco Moccia[1,8]✉

Colorectal carcinoma (CRC) represents the fourth most common cancer worldwide and is the third most common cause of malignancy-associated mortality. Distant metastases to the liver and lungs are the main drivers of CRC-dependent death. Pro-oxidant therapies, which halt disease progression by exacerbating oxidative stress, represent an antitumour strategy that is currently exploited by chemotherapy and ionizing radiation. A more selective strategy to therapeutically exploit reactive oxygen species (ROS) signaling would consist in targeting a redox sensor that is up-regulated in metastatic cells and is tightly coupled to the stimulation of cancer cell death programs. The non-selective cation channel, Transient Receptor Potential Ankyrin 1 (TRPA1), serves as a sensor of the cellular redox state, being activated to promote extracellular Ca^{2+} entry by an increase in oxidative stress. Recent work demonstrated that TRPA1 channel protein is up-regulated in several cancer types and that TRPA1-mediated Ca^{2+} signals can either engage an antiapoptotic pro-survival signaling pathway or to promote mitochondrial Ca^{2+} dysfunction and apoptosis. Herein, we sought to assess for the first time the outcome of TRPA1 activation by ROS on primary cultures of metastatic colorectal carcinoma (mCRC cells). We found that TRPA1 channel protein is up-regulated and mediates enhanced hydrogen peroxide (H_2O_2)-induced Ca^{2+} entry in mCRC cells as compared to non-neoplastic control cells. The lipid peroxidation product 4-hydroxynonenal (4-HNE) is the main ROS responsible for TRPA1 activation upon mCRC cell exposure to oxidative stress. TRPA1-mediated Ca^{2+} entry in response to H_2O_2 and 4-HNE results in mitochondrial Ca^{2+} overload, followed by mitochondrial depolarization and caspase-3/7 activation. Therefore, targeting TRPA1 could represent an alternative strategy to eradicate metastatic CRC by enhancing its sensitivity to oxidative stress.

Cell Death Discovery (2023)9:213 ; https://doi.org/10.1038/s41420-023-01530-x

INTRODUCTION

Colorectal carcinoma (CRC) represents the fourth most common cancer worldwide and is the third most common cause of malignancy-associated mortality, being responsible for 9.2% of fatalities among oncological patients (International Agency for Research on Cancer Available from: https://gco.iarc.fr/today, accessed 4th/04/2023). Involvement of secondary organs, such as the liver and lungs, is the main driver of CRC-dependent death: 25% of CRC patients show metastatic disease at diagnosis, whereas ≈50% of the patients develop disease recurrence within 5 years from surgery or adjuvant treatment [1]. The development of more effective strategies after the failure of conventional therapies for advanced/recurrent disease represents an unmet need for CRC patients. Reactive oxygen species (ROS), such as hydrogen peroxide (H_2O_2), have long been known to fuel tumor metastasis and invasion in a variety of cancer types [2], including mCRC [3]. Nevertheless, human clinical trials showed that dietary supplementation with antioxidants did not decrease, but rather enhanced, cancer incidence and cancer-related mortality [4]. Pro-oxidant therapies [2, 4], which halt disease progression by exacerbating oxidative stress in cancer cells, may represent an effective alternative antitumour strategy to current systemic treatments that are associated with a number of harmful side effects often leading to impaired quality of life, a worse overall prognosis and waste of health care resources [5]. A more selective strategy to exploit ROS signaling for therapeutic purposes would

[1]Department of Biology and Biotechnology "Lazzaro Spallanzani", University of Pavia, via Forlanini 6, 27100 Pavia, Italy. [2]Foundation IRCCS Policlinico San Matteo, Laboratory of Immunology Transplantation, Piazzale Golgi 19, Pavia, Italy. [3]Department of Molecular Medicine, University of Pavia, via Forlanini 6, 27100 Pavia, Italy. [4]Department of Biomedicine, School of Medicine, Benemérita Universidad Autónoma de Puebla, 13 Sur 2702 Colonia Volcanes, Puebla 72410, Mexico. [5]Department of Biosciences, Biotechnologies and Environment, University of Bari Aldo Moro, Via G. Amendola 165/A, 70125 Bari, Italy. [6]Medical Oncology, Foundation IRCCS Policlinico San Matteo, Piazzale Golgi 19, 27100 Pavia, Italy. [7]Department of Sciences Clinic-Surgical, Diagnostic and Pediatric, University of Pavia, Pavia, Italy. [8]These authors contributed equally: Daniela Montagna, Francesco Moccia. ✉email: d.montagna@smatteo.pv.it; francesco.moccia@unipv.it

Received: 13 April 2023 Revised: 5 June 2023 Accepted: 22 June 2023
Published online: 01 July 2023

consist in targeting a redox sensor that is up-regulated in neoplastic cells and is tightly coupled to the stimulation of cancer cell death programs.

Transient receptor potential ankyrin 1 (TRPA1) is a non-selective cation channel that is located within the plasma membrane and promotes extracellular Ca^{2+} entry in response to multiple chemical, physical, and thermal stimuli, thereby serving a polymodal sensor [6]. TRPA1 may serve as a ROS sensor due to the abundance of hyper-reactive cysteine residues that are located at the NH_2-terminal and can be oxidized by H_2O_2 [6, 7]. TRPA1 is the most abundant redox-sensitive TRP isoform in most cancer types [8], including invasive ductal breast carcinoma and lung adenocarcinoma, in which it supports H_2O_2-evoked intracellular Ca^{2+} oscillations and Ca^{2+}-dependent recruitment of pro-survival and antiapoptotic pathways to prevent ROS-induced cancer cell death [9]. Conversely, TRPA1-mediated increase in intracellular Ca^{2+} concentration ($[Ca^{2+}]_i$) supports H_2O_2-induced mitochondrial damage and apoptosis in other types of solid malignancies, such as glioblastoma multiforme [10, 11] and human oral squamous cell carcinoma (OSCC) [12]. A series of recent studies demonstrated that intracellular Ca^{2+} signals may either stimulate proliferation [13], inhibit the cell-cycle [14], or induce cell death [15] in primary cultures of metastatic CRC (mCRC) cells. The Ca^{2+} source dictates the outcome of $[Ca^{2+}]_i$ rise on cell fate, as distinct Ca^{2+}-permeable channels can be selectively coupled to different Ca^{2+}-dependent decoders in cancer cells [16, 17]. A further layer of complexity to the Ca^{2+}-dependent regulation of cancer hallmarks is added by the evidence that the same TRP isoform, e.g., TRP Vanilloid 1 (TRPV1), can exert opposing effects in different cancer types [18]. Therefore, understanding whether TRPA1-mediated Ca^{2+} entry stimulates or rather prevents ROS-dependent mCRC dell death is mandatory to design alternative therapies based upon the manipulation of TRPA1 activity to sensitize mCRC cells to oxidative stress.

RESULTS

TRPA1 protein is up-regulated and mediates enhanced Ca^{2+} entry in mCRC cells

Preliminary evidence indicates that *TRPA1* gene is expressed in CRC [19], but it is still unknown whether it is translated into a functional protein in mCRC cells. Immunoblots identified a major band of ~140 kDa in both primary cultures of mCRC and control cells isolated from adjacent non-neoplastic tissue (Fig. 1A and Fig. S1), as also observed in other cancer cell types [20, 21], and densitometric analysis revealed that TRPA1 protein was significantly ($p < 0.05$) up-regulated in mCRC cells (Fig. 1B). In order to assess whether TRPA1 protein was able to mediate extracellular Ca^{2+} entry, both cell types were loaded with the Ca^{2+}-sensitive fluorophore, Fura-2 acetoxymethyl ester (Fura-2/AM), as described elsewhere [14, 22]. TRPA1 stimulation by the selective electrophilic agonist, allyl isothiocyanate (AITC; 30 μM) induces larger intracellular Ca^{2+} signals in primary cultures of mCRC cells as compared to non-neoplastic cells (Fig. 1C, D). Interestingly, AITC induced a sustained Ca^{2+} overload in mCRC cells (Fig. 1A, blue tracing), which is a hallmark of pro-apoptotic Ca^{2+} signals [11, 23], while it evoked low-amplitude intracellular Ca^{2+} oscillations in non-neoplastic cells (Fig. 1C; red tracing), which could rather exert a mitogenic effect [13, 24]. AITC failed to increase $[Ca^{2+}]_i$ in the absence of extracellular Ca^{2+} ($0Ca^{2+}$) (Fig. S2), while restoring extracellular Ca^{2+} concentration (1.5 mM) caused an immediate and long-lasting elevation in $[Ca^{2+}]_i$ in mCRC cells (Fig. S2). Therefore, the Ca^{2+} response to AITC is mainly mediated by extracellular Ca^{2+} entry. In order to confirm that TRPA1 mediates AITC-evoked Ca^{2+} influx, mCRC cells were pretreated with HC-030031 (30 μM), which represents the most widespread used TRPA1 inhibitor [6, 7, 21, 23]. As expected, HC-030031 significantly ($p < 0.05$) reduced both the amplitude and the duration of the Ca^{2+} response to AITC (Fig. 2A, B). In addition, genetic silencing of TRPA1 expression with a selective small interfering RNA (siTRPA1)

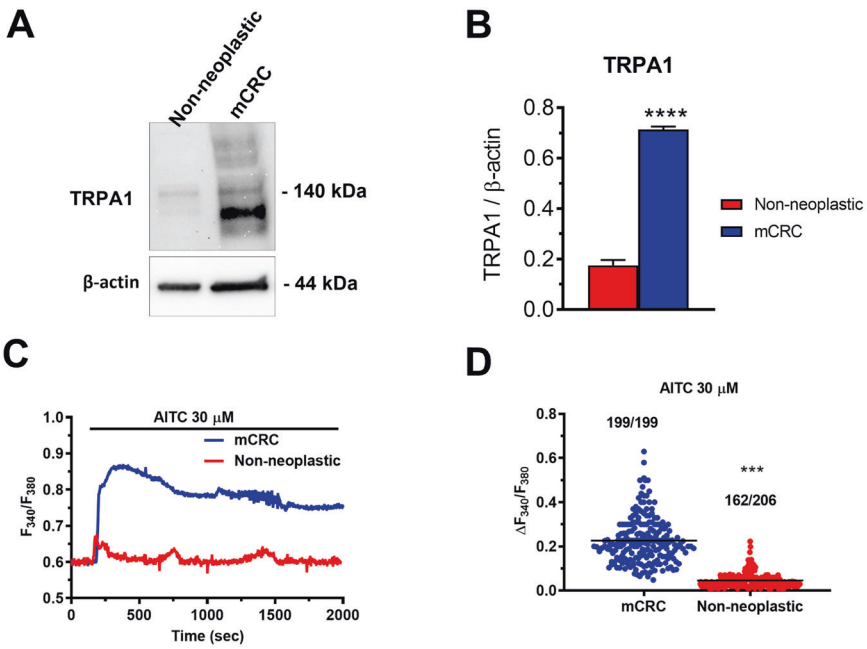

Fig. 1 TRPA1 protein is up-regulated and mediates enhanced Ca^{2+} signaling in primary cultures of mCRC cells. A TRPA1 protein expression in non-neoplastic cells and primary cultures of mCRC cells. Blots representative of four independent experiments (each conducted on samples deriving from a distinct patient) were shown. Major bands of the predicted molecular weights for TRPA1 and β-actin proteins were indicated. **B** Mean ± SE of TRPA1 protein expression in non-neoplastic and mCRC cells. The results were normalized to the corresponding β-actin (****$p < 0.0001$; Student's *t*-test). TRPA1 protein was significantly more expressed in mCRC cells. **C** The selective TRPA1 agonist, AITC (30 μM), evoked intracellular Ca^{2+} signals in mCRC and non-neoplastic cells. **D** Mean ± SE of the amplitude of the peak Ca^{2+} response (scattered dot plot) to AITC in both mCRC and non-neoplastic cells. Student's *t*-test: ***$p < 0.001$. The numbers placed above the scattered dots represent the number of responding cells out of the total cell number. $N = 4$ for each experimental condition.

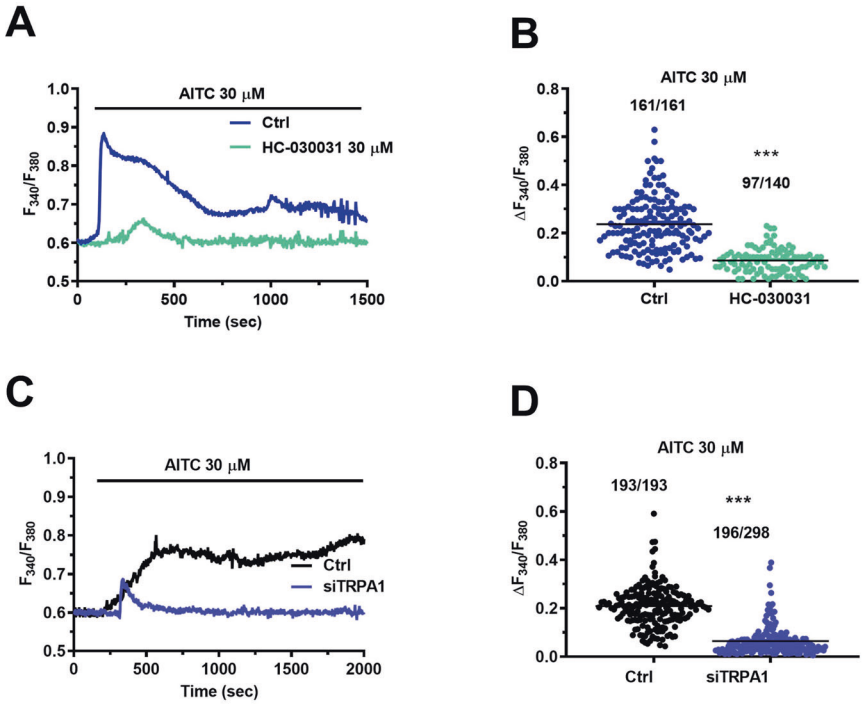

Fig. 2 TRPA1 channel mediates AITC-evoked Ca^{2+} entry in primary cultures of mCRC cells. A Intracellular Ca^{2+} signals induced by 30 μM AITC (Ctrl) were abrogated upon pre-treating mCRC cells with the specific TRPA1 inhibitor, HC-030031 (30 μM, 30 min). **B** Mean ± SE of the peak Ca^{2+} signal evoked by AITC in the absence (Ctrl) and presence of HC-030031. **C** Intracellular Ca^{2+} signals induced by 30 μM AITC in mCRC cells transfected with a scrambled construct (Ctrl) or with a selective siTRPA1. **D** Mean ± SE of the amplitude of Ca^{2+} response to AITC under the designated treatment. Student's *t*-test: ***$p < 0.001$. The placed above the scattered dots represent the number of responding cells out of the total cell number. $N = 4$ for each experimental condition.

significantly ($p < 0.05$) reduced AITC-evoked extracellular Ca^{2+} entry in mCRC cells (Fig. 2C, D). The efficacy of TRPA1 deletion in mCRC cells by the siTRPA1 was confirmed by comparing TRPA1 protein expression in mCRC cells transfected with the selective siTRPA1 and with a scrambled construct (Figs. S3 and S4). Altogether, these data show that TRPA1 protein is up-regulated and mediated extracellular Ca^{2+} entry in primary cultures of mCRC cells.

TRPA1 mediates H_2O_2-induced Ca^{2+} signals in mCRC cells

In cancer cells, H_2O_2 may either stimulate ROS-dependent apoptosis [11] or engage an anti-oxidant defense program through intracellular Ca^{2+} signaling. Preliminary Ca^{2+} imaging recordings showed that H_2O_2 induced a dose-dependent increase in $[Ca^{2+}]_i$ (Fig. S5A), which presented a minimum effective dose of 1 μM, a half-maximal effective concentration (EC_{50}) of 35.37 μM, and a maximal response at 200 μM (Fig. S5B). Low micromolar doses of H_2O_2 (10–25 μM) induced low-amplitude intracellular Ca^{2+} oscillations (Fig. S5A), while higher doses evoked a potentially cytotoxic Ca^{2+} overload (Figure S5A), as previously described for AITC (Fig. 1C, blue tracing). H_2O_2 concentration within cancer microenvironment may rise to 50 μM [25]. The Ca^{2+} response to 50 μM H_2O_2 was significantly ($p < 0.05$) larger in mCRC cells as compared to non-neoplastic cells (Fig. 3A, B). Furthermore, the prolonged increase in $[Ca^{2+}]_i$ evoked by 50 μM H_2O_2 in mCRC cells was dampened by pharmacological (via 30 μM HC-030031) and genetic (via the selective siTRPA1) blockade of TRPA1 (Fig. 3C and Fig. 3D). In addition, the Ca^{2+} response to was sensitive to dithiothreitol (DTT) (5 mM) (Fig. 3E, F), a thiol-reducing compound that reverses H_2O_2-dependent Ca^{2+} signals [26, 27], and to the H_2O_2 scavenger, catalase (500 U/mL) (Fig. 3E, F) [26, 28]. Oxidative stress in cancer microenvironment may result in the peroxidation of ω6 polyunsaturated fatty acids in the plasma membrane, thereby leading to the formation of 4-hydroxy-nonenal (4-HNE) [9, 29]. 4-HNE has recently been shown to stimulate TRPA1-mediated Ca^{2+} influx in several cell types [30, 31], including melanoma cell lines [29]. Fifty μM H_2O_2-evoked Ca^{2+} overload in mCRC cells was abolished by deferoxamine (100 μM) (Fig. 3E, F), which prevents H_2O_2 degradation into the hydroxyl radical ($OH^{\bullet}$) [26, 31]. Furthermore, exogenous administration of 4-HNE (30 μM) induced a slowly rising and protracted increase in $[Ca^{2+}]_i$ that was sensitive to TRPA1 inhibition with HC-030031 (30 μM) (Fig. 3G, H). Therefore, these data demonstrated that high concentrations of H_2O_2 induced cytosolic Ca^{2+} overload via 4-HNE-dependent TRPA1 activation in mCRC cells.

TRPA1 mediates H_2O_2-induced mitochondrial dysfunction and caspase-3/7 activation in mCRC cells

In order to assess whether H_2O_2-induced TRPA1 activation affect mCRC cell viability, we exploited the Trypan blue exclusion assay [14]. AITC (30 μM) and H_2O_2 (50 μM) caused a significant ($p < 0.05$) reduction in the percentage of viable cells at 24 h, 48 h, and 72 h (Fig. S6A, C, respectively). However, the pharmacological blockade of TRPA1 with HC-030031 (30 μM) rescued viability in mCRC cells exposed both to AITC (Fig. S6A) and H_2O_2 (Fig. S6C). The reduction in cell viability was associated to a significant ($p < 0.05$) decrease in cell growth that was rescued by blocking TRPA1-mediated Ca^{2+} influx with HC-030031 (30 μM) (Fig. S6B, S6D for AITC and H_2O_2, respectively). Conversely, stimulating TRPA1 with either AITC (30 μM) or H_2O_2 (50 μM) did not affect viability (Fig. S6E) and cell growth (Fig. S6F) in non-neoplastic cells. Therefore, these preliminary findings indicate that TRPA1-mediated Ca^{2+} influx affects viability in primary cultures of mCRC cells, but not in their normal counterparts.

We then evaluated whether TRPA1 activation in mCRC cells leads to apoptosis. A hallmark of apoptotic cell death is represented by mitochondrial Ca^{2+} overload, which causes mitochondrial depolarization and opening of the mitochondrial permeability transition pore (mPTP) followed by caspase-3/7 activation [32–34]. The ROS-dependent increase in mitochondrial

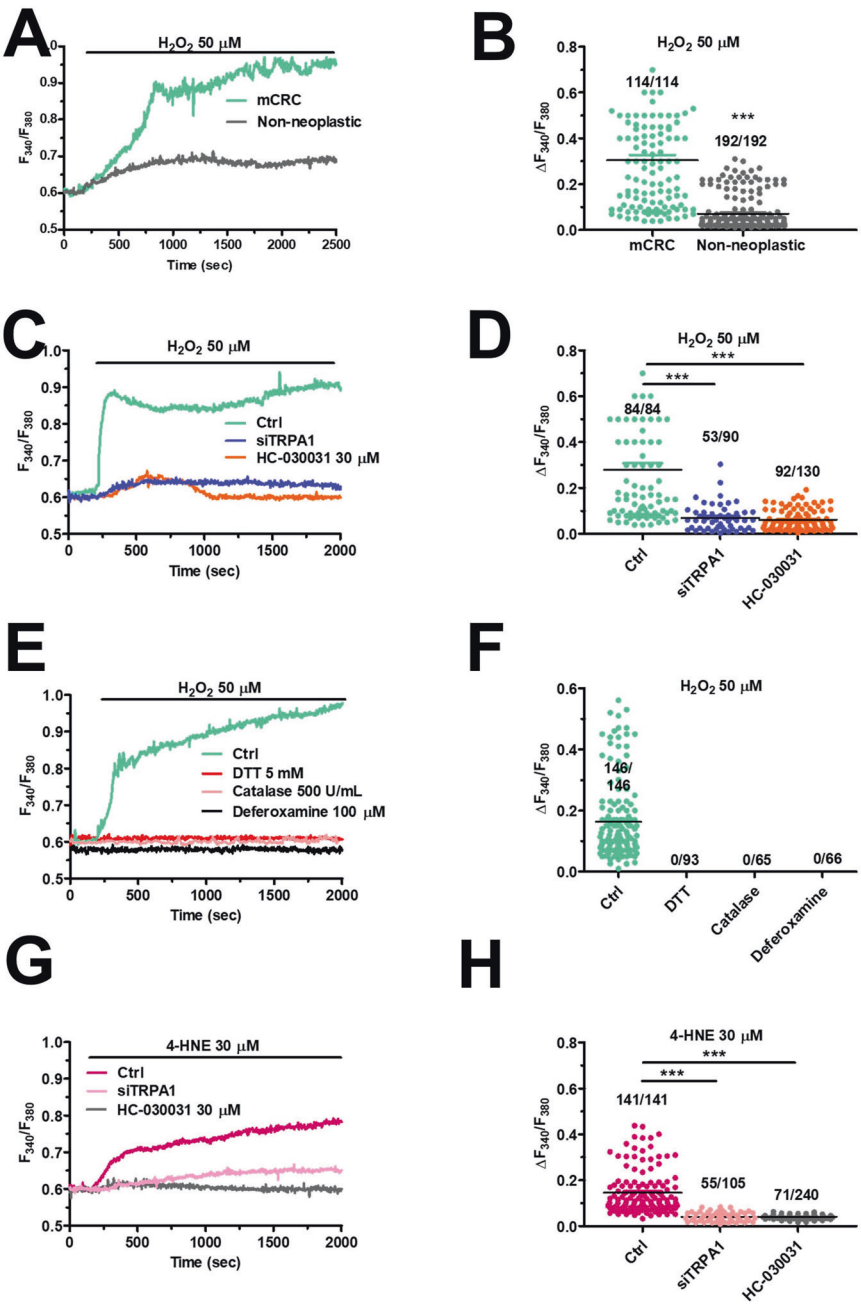

Fig. 3 TRPA1 mediates H_2O_2-induced intracellular Ca^{2+} signals in primary cultures of mCRC cells. A H_2O_2 (50 μM) induces larger Ca^{2+} signals in mCRC as compared to non-neoplastic cells. **B** Mean ± SE of peak Ca^{2+} signal evoked by H_2O_2 in both mCRC and non-neoplastic cells. Student's *t*-test: ***$p < 0.001$. The placed above the scattered dots represent the number of responding cells out of the total cell number. $N = 4$ for each experimental condition. **C** Intracellular Ca^{2+} signals induced by 50 μM H_2O_2 (Ctrl) were abrogated in mCRC cells pretreated with the specific TRPA1 inhibitor, HC-030031 (30 μM, 30 min), or transfected with the selective siTRPA1. **D** Mean ± SE of the peak Ca^{2+} signal evoked by H_2O_2 in control (Ctrl) mCRC cells and in mCRC cells transfected with siTRPA1 or pretreated with HC-030031. One-way ANOVA followed by the post hoc Dunnett's test: ***$p < 0.001$. The numbers placed above the scattered dots represent the number of responding cells out of the total cell number. $N = 4$ for each experimental condition. **E** Intracellular Ca^{2+} signals induced by 50 μM H_2O_2 in the absence (Ctrl) and presence of the thiol-reducing compound, DTT (5 μM), the H_2O_2 scavenger, catalase (500 U/mL) or the iron-chelating compound, deferoxamine (100 μM). **F** Mean ± SE of peak Ca^{2+} signal evoked by H_2O_2 under the designated treatments. The numbers placed above the scattered dots represent the number of responding cells out of the total cell number. $N = 4$ for each experimental condition. **G** Intracellular Ca^{2+} signals induced by the selective TRPA1 agonist, 4-HNE (30 μM), in mCRC cells under control conditions (Ctrl) or upon pharmacological (HC-030031; 30 μM, 30 min) or genetic (with a selective siTRPA1) blockade of TRPA1 activity. **H** Mean ± SE of peak Ca^{2+} signal evoked by 4-HNE in control (Ctrl) mCRC cells and in mCRC cells treated with DTT, catalase, and deferoxamine. One-way ANOVA followed by the post hoc Dunnett's test: ***$p < 0.001$. The numbers placed above the scattered dots represent the number of responding cells out of the total cell number. $N = 4$ for each experimental condition.

Ca^{2+} concentration ($[Ca^{2+}]_{mito}$) was evaluated in mCRC cells loaded with Rhod-2/AM, the most widely employed fluorophore to monitor mitochondrial free Ca^{2+} levels [32, 34, 35]. AITC (30 μM) evoked a long-lasting elevation in $[Ca^{2+}]_{mito}$ that was abolished by blocking TRPA1 with either HC-030031 (30 μM) or the selective siTRPA1 and by inhibiting mitochondrial Ca^{2+} uptake with the specific antagonist Ru360 (5 μM) [35] (Fig. 4A, B). Also, 50 μM H_2O_2 (Fig. 4C, D) and 30 μM 4-HNE (Fig. 4E, 4F) induced a protracted

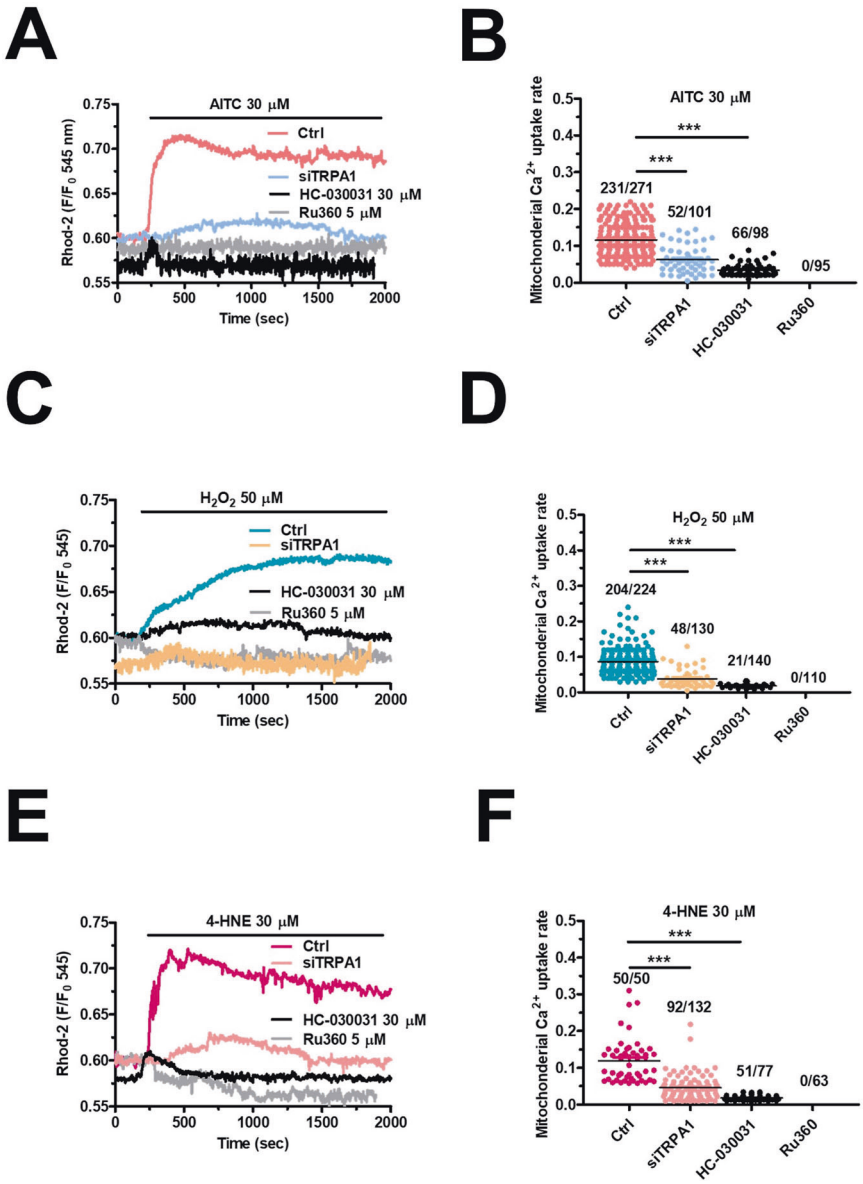

Fig. 4 TRPA1 activation induces mitochondrial Ca^{2+} overload in primary cultures of mCRC cells. A Mitochondrial Ca^{2+} signals induced by AITC (30 μM) in mCRC cells maintained under control conditions (Ctrl), pretreated with HC-030031 (30 μM, 30 min) or with the highly specific inhibitor of the mitochondrial Ca^{2+} uniporter, Ru360 (5 μM, 30 min), or transfected with the selective siTRPA1. **B** Mean ± SE of peak mitochondrial Ca^{2+} signal evoked by AITC in control (Ctrl) mCRC cells and in mCRC cells transfected with siTRPA1 or pretreated with HC-030031 or Ru360. One-way ANOVA followed by the post hoc Dunnett's test. ***$p < 0.001$. The numbers placed above the scattered dots represent the number of responding cells out of the total cell number. $N = 4$ for each experimental condition. **C** Mitochondrial Ca^{2+} signals induced by H_2O_2 (50 μM) in mCRC cells maintained under control conditions (Ctrl), pretreated with HC-030031 (30 μM, 30 min) or with the highly specific inhibitor of the mitochondrial Ca^{2+} uniporter, Ru360 (5 μM, 30 min), or transfected with the selective siTRPA1. **D** Mean ± SE of peak mitochondrial Ca^{2+} signal evoked by H_2O_2 in control (Ctrl) mCRC cells and in mCRC cells transfected with siTRPA1 or pretreated with HC-030031 or Ru360. One-way ANOVA followed by the post hoc Dunnett's test. ***$p < 0.001$. The numbers placed above the scattered dots represent the number of responding cells out of the total cell number. $N = 4$ for each experimental condition. **E** Mitochondrial Ca^{2+} signals induced by 4-HNE (30 μM) in mCRC cells maintained under control conditions (Ctrl), pretreated with HC-030031 (30 μM, 30 min) or with the highly specific inhibitor of the mitochondrial Ca^{2+} uniporter, Ru360 (5 μM, 30 min), or transfected with the selective siTRPA1. **F** Mean ± SE of peak mitochondrial Ca^{2+} signal evoked by 4-HNE in control (Ctrl) mCRC cells and in mCRC cells transfected with siTRPA1 or pretreated with HC-030031 or Ru360. One-way ANOVA followed by the post hoc Dunnett's test. ***$p < 0.001$. The numbers placed above the scattered dots represent the number of responding cells out of the total cell number. $N = 4$ for each experimental condition.

elevation in $[Ca^{2+}]_{mito}$ that was sensitive to the genetic or pharmacological blockade of TRPA1-mediated Ca^{2+} entry and to the pharmacological blockade of mitochondrial Ca^{2+} uptake. Consistently, exposure to 30 μM AITC (Fig. 5A), 50 μM H_2O_2 (Fig. 5A), and 30 μM 4-HNE (Fig. 5A) caused significant ($p < 0.05$) mitochondrial depolarization, which was rescued by blocking TRPA1-mediated Ca^{2+} entry with either HC-030031 (30 μM) or the selective siTRPA1 (Fig. 5A). We finally assessed whether TRPA1-mediated mitochondrial Ca^{2+} overload results in caspase activation in mCRC cells loaded with the with the caspase-3/7-sensitive DEVD-based dye CellEvent [36, 37]. Single-cell imaging revealed that both AITC (30 μM) and H_2O_2 (50 μM) caused a significant increase in caspase-3/7 activation at, respectively, ~12.5 and ~7.5 h, which was maintained until the end of the recording

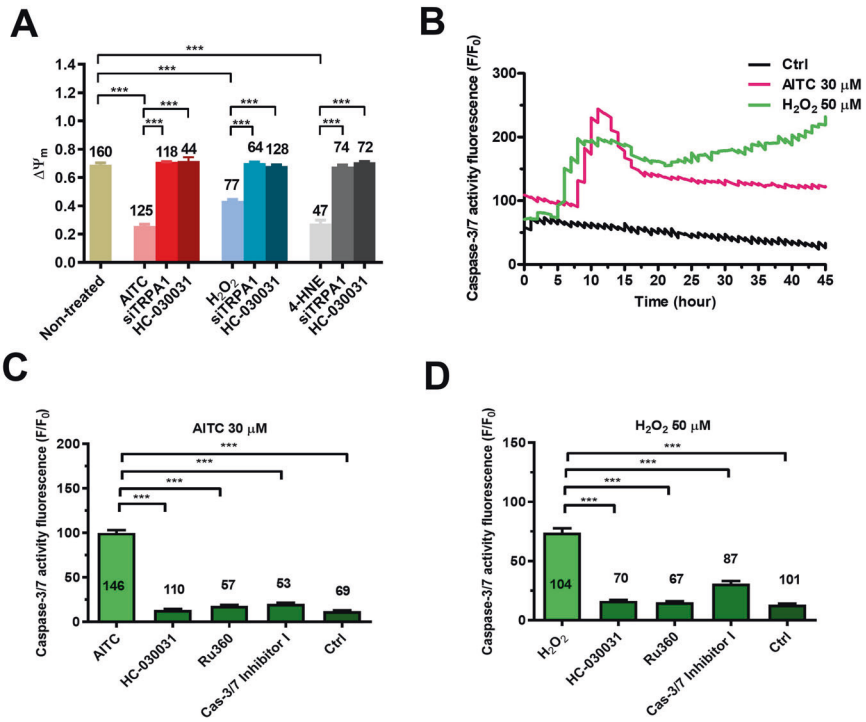

Fig. 5 TRPA1-mediated extracellular Ca^{2+} entry causes mitochondrial depolarization and caspase-3/7 activation in mCRC cells. **A** Mean ± SE of $\Delta\Psi_m$ measured under control conditions (Ctrl) and after the following treatments: (1) AITC (30 μM, 6 h); AITC (30 μM, 6 h) + HC-030031 (30 μM, 30 min); AITC (30 μM, 6 h) + siTRPA1; (2) H_2O_2 (50 μM, 6 h); H_2O_2 (50 μM, 6 h) + HC-030031 (30 μM, 30 min); H_2O_2 (50 μM, 6 h) + siTRPA1; (3) 4-HNE (30 μM, 6 h); 4-HNE (30 μM, 6 h) + HC-030031 (30 μM, 30 min); 4-HNE (30 μM, 6 h) + siTRPA1. One-way ANOVA followed by the post hoc Dunnett's test. ***$p < 0.001$. The numbers placed above the histogram bars represent the number of responding cells out of the total cell number. $N = 4$ for each experimental condition. $\Delta\Psi_m$ was measured by evaluating tetramethyl rhodamine methyl ester (TMRM) fluorescence. **B** Tracings show the changes in CellEvent™ fluorescence, signifying caspase-3/7 activation, in the absence (Ctrl) and presence of either AITC (30 μM) or H_2O_2 (50 μM). Each tracing is representative of 113 cells (Ctrl), 91 cells (AITC), and 86 cells (H_2O_2) from 3 independent experiments. Every recording lasted 45 h at a sampling rate of 1 image/15 min. **C** Mean ± SE of CellEvent™ fluorescence intensity under the following conditions: Control (Ctrl); AITC (30 μM, 6 h); AITC (30 μM, 6 h) + HC-030031 (30 μM, 30 min); AITC (30 μM, 6 h) + Ru360 (5 μM, 30 min); AITC (30 μM, 6 h) + Caspase-3/7 Inhibitor I (20 μM, 30 min). One-way ANOVA followed by the post hoc Dunnett's test. ***$p < 0.001$. The numbers placed above the histogram bars represent the number of responding cells out of the total cell number. $N = 4$ for each experimental condition. **D** Mean ± SE of CellEvent™ fluorescence intensity under the following conditions: Control (Ctrl); H_2O_2 (50 μM, 6 h); H_2O_2 (50 μM, 6 h) + HC-030031 (30 μM, 30 min); H_2O_2 (50 μM, 6 h) + Ru360 (5 μM, 30 min); H_2O_2 (50 μM, 6 h) + Caspase-3/7 Inhibitor I (20 μM, 30 min). One-way ANOVA followed by the post hoc Dunnett's test. ***$p < 0.001$. The numbers placed above the histogram bars represent the number of responding cells out of the total cell number. $N = 4$ for each experimental condition.

period (45 h) (Fig. 5B and Fig. S7A). Caspase-3/7 activation was suppressed by blocking TRPA1 with HC-03031 (30 μM), by inhibiting MCU with Ru360 (5 μM), and by preventing caspase-3/7 activation with Caspase-3/7 Inhibitor I (20 μM) (Fig. 5C for AITC and Fig. 5D for H_2O_2; see also Fig. S7B for both agonists). These findings indicate that TRPA1-mediated Ca^{2+} influx supports H_2O_2-induced mCRC cell apoptotic death by causing mitochondria dysfunction and caspase-3/7 activation.

DISCUSSION

In this investigation, we demonstrated for the first time that the redox-sensitive TRPA1 channel is up-regulated, mediates enhanced Ca^{2+} entry and thereby leads to mitochondrial dysfunction and caspase-3/7 activation in primary cultures of mCRC. Therefore, TRPA1 stimulation could represent an alternative therapeutic approach to sensitize mCRC to ROS-dependent cell death [38].

TRPA1 is emerging as the primary redox-sensitive TRP isoform in cancer microenvironment [7–9]. TRPA1 protein is up-regulated in multiple solid malignancies, such as invasive ductal breast carcinoma and lung adenocarcinoma [9], OSCC [12], pancreatic adenocarcinoma [20], and prostate cancer [21]. The outcome of TRPA1 stimulation by oxidative stress may vary depending on the tumor type: for instance, TRPA1-mediated Ca^{2+} entry engages a non-canonical anti-oxidant defense program in lung and breast cancers [8, 9], while it stimulates mitochondrial dysfunction and apoptosis in glioblastoma multiforme [10, 11]. Herein, we found that TRPA1 protein expression was remarkably enhanced in primary cultures of mCRC cells, which represent a suitable model to investigate the impact of intracellular Ca^{2+} signals on a therapeutically relevant model of human CRC [13–15, 39, 40], as compared to non-neoplastic cells. In addition, the electrophilic TRPA1 agonist, AITC, evoked a sustained increase in $[Ca^{2+}]_i$ that was sensitive to both pharmacological (via HC-030031) and genetic blockade of TRPA1 activity (via a selective siTRPA1). The waveform of this Ca^{2+} response is quite different from the repetitive oscillations in $[Ca^{2+}]_i$ evoked by TRPA1 activation in lung and breast cancer cells [9]. Interestingly, intracellular Ca^{2+} oscillations in cancer cells have long been known to stimulate cell proliferation and survival [41, 42], while long-lasting elevations in $[Ca^{2+}]_i$ lead to apoptotic cell death [32, 41, 43]. In accord, AITC-evoked cytosolic Ca^{2+} overload reduced viability in OSCC cells [12].

Similar to AITC, mid-to-high micromolar concentrations of H_2O_2 evoked a long-lasting increase in $[Ca^{2+}]_i$, which was inhibited by blocking TRPA1-mediated Ca^{2+} entry via either HC-030031 or the selective siTRPA1. Reactive lipid mediators generated by lipid

peroxidation of polyunsaturated fatty acids in the plasma membrane, such as 4-HNE, are involved in cancer initiation and progression [9, 29, 44]. TRPA1 is highly sensitive to 4-HNE [30, 31] and 4-HNE-induced TRPA1 activation has been reported in melanoma cell lines [29]. In the presence of iron, H_2O_2 is degraded into $OH^{\cdot}$ via the Fenton reaction, thereby inducing lipid peroxidation and 4-HNE formation [45, 46]. Of note, the Ca^{2+} response to H_2O_2 was abolished by preventing the Fenton reaction with deferoxamine. In addition, exogenous administration of 4-HNE caused a cytosolic Ca^{2+} overload in mCRC cells that resembled those induced by AITC and H_2O_2 and was dependent on TRPA1 activation. These findings strongly indicate that 4-HNE is the more likely agonist to induce TRPA1 activation by oxidative stress in mCRC cells. Moreover, the long-lasting Ca^{2+} elevation resulting from TRPA1 stimulation in mCRC cells is seemingly more suitable to stimulate mitochondrial dysfunction and apoptotic cell death rather than promoting cell proliferation or survival. In accord, prolonged exposure of primary cultures of mCRC cells to AITC and H_2O_2 reduced their viability and proliferation rate in a TRPA1-dependent manner. Furthermore, stimulation with AITC, H_2O_2, and 4-HNE caused mitochondrial Ca^{2+} overload that was suppressed by the pharmacological and genetic blockade of TRPA1-mediated extracellular Ca^{2+} entry. This is the first evidence that TRPA1 activation leads to mitochondrial Ca^{2+} uptake in cancer cells. However, previous studies showed that TRPA1 mediates ROS-induced mitochondrial Ca^{2+} entry in OLN-93 oligodendrocytes [47] and THP-1-derived macrophages [48]. In both cell types, TRPA1-dependent mitochondrial Ca^{2+} overload led to mitochondrial depolarization and apoptotic cell death [47, 48]. In accord, aberrant mitochondrial Ca^{2+} rise induces mPTP opening and thereby leads to the dissipation of the mitochondrial membrane potential and the release of pro-apoptotic factors that activate the executioner caspase-3 and caspase-7 [33, 49, 50]. Similarly, we first found that stimulation of TRPA1 with AITC, H_2O_2, and 4-HNE caused a significant reduction in mitochondrial membrane potential in mCRC cells. Then, by using the commercial kit CellEvent™ Caspase-3/7 Green Detection Reagent [36, 37], we demonstrated that AITC and H_2O_2 evoked an early increase in caspase-3/7 activation, which was suppressed by inhibiting TRPA1-mediated Ca^{2+} entry. Likewise, TRPA1 was found to mediate oxidative stress-dependent caspase-3 activation and apoptosis in temozolomide-treated SH-SY5Y neuroblastoma cells [51] and in mouse retina undergoing ischemia-reperfusion injury [52]. Therefore, TRPA1 activation in mCRC cells supports ROS-dependent apoptosis rather than cell survival, as otherwise reported in breast and lung cancers [8, 9].

The distinct outcome of ROS-dependent TRPA1 activation in different cancer types, e.g., survival in breast and lung cancers [8, 9] and apoptosis in mCRC and glioblastoma multiforme [11], is likely to be associated to the heterogeneity of TRPA1-mediated Ca^{2+} signals. Takahashi and coworkers reported that H_2O_2 evoked intracellular Ca^{2+} oscillations in several breast and lung cancer cell lines. These repetitive Ca^{2+} transients in turn recruit the Ca^{2+}/Calmodulin-dependent protein tyrosine kinase 2 (PYK2), which engages the anti-oxidant and antiapoptotic signaling pathways that protect cancer cells from oxidative stress [8, 9]. Of note, repetitive oscillations in $[Ca^{2+}]_i$ are nicely suited to recruit Ca^{2+}-dependent effectors that promote cancer cell proliferation and survival, including Pyk2 [24, 53, 54], while avoiding mitochondrial Ca^{2+} overload [55]. It is still to understand why TRPA1-mediated Ca^{2+} entry does not result in repetitive Ca^{2+} spikes also in mCRC cells. The spiking Ca^{2+} response observed in breast and cancer cell lines resembles the inositol-1,4,5-trisphosphate-evoked Ca^{2+} release events from the endoplasmic reticulum (ER) that could be triggered by Ca^{2+} entry through TRP channels via the Ca^{2+}-induced Ca^{2+} release process [26, 56]. Future work will have to examine the possibility that TRPA1 channels on the plasma membrane are juxtaposed to ER-located inositol-1,4,5-trisphosphate receptors in some, e.g., lung and breast cancers, but not all solid malignancies.

CONCLUSIONS

Our results show that the redox-sensitive TRPA1 channel is up-regulated and mediates enhanced extracellular Ca^{2+} entry in mCRC cells as compared to non-neoplastic controls. The enhanced expression of TRPA1 results in cytosolic Ca^{2+} overload in mCRC cells exposed to H_2O_2 and this influx of Ca^{2+} is likely to depend on H_2O_2 degradation to $OH^{\cdot}$ and subsequent formation of the lipid peroxidation-derived 4-HNE. ROS-dependent TRPA1 activation in turn causes mitochondrial Ca^{2+} overload and thereby leads to mitochondrial depolarization and caspase-3/7 activation. Therefore, TRPA1 activation contributes to ROS-dependent mCRC apoptosis. These findings suggest that TRPA1 stimulation could represent a promising therapeutic avenue to sensitize mCRC cell to oxidative stress, possibly in combination with pro-oxidant therapies [2, 4].

MATERIALS AND METHODS

Isolation and expansion of mCRC cells from CRC patients

Primary mCRC cells were isolated and expanded how illustrated in [15, 39, 40]. Patients (>18 years) suffering mCRC, previously undergoing surgery intervention to excise primary CRC tumor and/or liver metastases, signed an informed consent before being enrolled. The whole procedure was carried out in according with the rules of the revised (2013) Declaration of Helsinki of 1975 (https://www.wma.net/what-we-do/medical-ethics/declaration-of-helsinki/). The Foundation IRCCS Policlinico San Matteo in Pavia (Italy) (Ethical code 20110000996, 17/01/2011) approved the present investigation. Tumor specimens were treated by using in combination the Tumor dissociation Kit (Miltenyi Biotec, Bologna, Italy; cat# 130-095-929) and the GentleMACS Dissociator (Miltenyi Biotec, Bologna, Italy, cat# 130-093-235) to rapidly generated single-cell suspensions [15, 39, 40]. Subsequently, clusters of mCRC cells were removed through filtration, and the cells were resuspended at a concentration of $0.5–1 \times 10^6$ cells/mL in CellGro SCGM medium (Cell Genix, Freiburg, Germany, cat# 20802-0500), which was supplemented with 0.1% gentamycin (Gibco, Life Technologies Limited, Paisley, UK, cat# 15750-037) and 20% foetal bovine serum (FBS) (Euroclone, Pero, Mi, Italy; cat# ECS0180D) (complete medium), seeded and expanded in 25 cm^2 tissue flasks (Corning, Stone Staffordshire, England, cat# 430639) in a CO_2 incubator. The adherent cells were evaluated microscopically every 24–48 h and when they reached about 70% confluence were trypsinized, washed and cryopreserved in 90% FBS and 10% dimethyl sulfoxide (DMSO) for later use. To confirm that the isolated cells derived from neoplastic specimens, at least 3 cytospins were carried out exploiting 10^5 cultured cells/cytospin deriving from 4–6 passages, for morphologic and immunocytochemical characterization, as described in [14, 39].

Solutions to measure changes in $[Ca^{2+}]_i$

Physiological salt solution (PSS) consisted of (in mM): 150 NaCl, 6 KCl, 1.5 $CaCl_2$, 1 $MgCl_2$, 10 Glucose, 10 Hepes. A Ca^{2+}-free solution ($0Ca^{2+}$) was obtained by replacing $CaCl_2$ with 2 mM NaCl and adding 0.5 mM EGTA. NaOH was used to titrate solutions to pH 7.4. An osmometer (Wescor 5500, Logan, UT) was used to measure the osmolality of the solutions, which was found to be 338 mmol/kg.

Intracellular Ca^{2+} imaging

TRPA1-mediated changes in $[Ca^{2+}]_i$ were monitored in mCRC and non-neoplastic cells loaded with the Ca^{2+}-sensitive ratiometric indicator, Fura-2 acetoxymethyl ester (Fura-2/AM) [40]. The cells were plated on round glass coverslips (8 mm diameter) coated with collagen (5 mg/mL; Sigma), bathed with PSS, loaded with 4 μM Fura-2 and then maintained in the presence of the Ca^{2+} indicator for 30 min at 37 °C and 5% CO_2. Subsequently, the cells were extensively washed with fresh PSS and the coverslip was gently attached to the bottom of a Petri dish with silicon grass (Saratoga, Trezzano sul Naviglio, Mi, Italy). The Petri dish was then moved on the stage of an upright epifluorescence Axiolab microscope (Carl Zeiss, Oberkochen, Germany) and the cells were observed with a Zeiss × 40 Achroplan objective (water-immersion, 0.9 numerical aperture, 2.0 mm working distance). Every 3 sec, Fura-2 was alternately (0.5 Hz) excited at 340 and 380 nm, and the emitted fluorescence was recorded at 510 nm. A filter wheel (Lambda 10, Sutter Instrument, Novato, CA, USA) was used to accommodate the excitation filters. 10–40 rectangular "regions of interest" (ROI) were drawn around the cells that were clearly identifiable in the visual field. At each excitation wavelength, images of the visual field and the fluorescence within each ROI were acquired

by an Extended-ISIS Camera (Photonic Science, Millham, UK). A custom software that was working in the LINUX environment was employed to control both the Extended-ISIS Camera and the filter wheel. The LINUX-based software was also used to measure the ratio of the mean fluorescence emitted at 510 nm when the cells within each ROI were excited alternatively at 340 and 380 nm (F_{340}/F_{380}). All recordings were carried out at room temperature (22 °C).

Mitochondrial Ca^{2+} measurement

Mitochondrial Ca^{2+} was evaluated with Rhod-2/AM by using the same single-cell imaging set-up used to detect variations in Fura-2 fluorescence. Rhod-2 is excited at 545 nm and emits fluorescence at 590 nm. Therefore, changes in Rhod-2 fuorescence were measured by using a TRITC filter cube. The mCRC cells were incubated in PSS containing 4 µM Rhod-2/AM for 45 min at 37 °C and 5% CO_2. Subsequently, the cells were extensively washed with fresh PSS and the coverslip was attached to the bottom of a Petri dish, as described above for Fura-2. Recordings were performed and plotted on-line every 3 sec. All the recordings were carried out at 22 °C.

Measurement of mitochondrial membrane potential ($\Delta\Psi_m$)

$\Delta\Psi_m$ was measured as recently described [14], by incubating mCRC cells in PSS containing 25 nM TMRM and 200 nM Cyclosporine H for 30 min at 37 °C and 5% CO_2. Changes in TMRM fluorescence were recorded by using the same imaging set-up employed to record TRPA1-mediated increases in Fura-2 and Rhod-2 fluorescence. The TMRM red-orange fluorescence (excitation 480 nm, emission 510 nm) was measured with the aid of a TRITC filter cube for live imaging. A round diaphragm was exploited to increase the contrast. Recordings were carried out and plotted on-line every 10 s. The experiments were performed at 22 °C.

Measurement of caspase-3/7 activity

Intracellular caspase-3/7 activity was evaluated by single-cell fluorescence microscopy by using the CellEvent™Caspase-3/7 Green Detection Reagent according to the manufacturer's intructions (Thermofisher Scientific, Rodano, Mi, Italy). This reagent consists of a four-amino acid peptide (DEVD) conjugated to a nucleic acid-binding dye, which is non-fluorescent when it is not bound to DNA. The DEVD peptide sequence is a cleavage site for caspase-3/7 and, therefore, upon caspase-3/7 activation in apoptotic cells, the free dye can bind to DNA and emit bright green fluorescence. Cells were seeded in 12-well plates (Corning, Stone Staffordshire, England; cat#3513) and, upon reaching 70% confluence, were loaded with the CellEvent™ Caspase-3/7 Green Detection Reagent (5 µM) for 30 min at 37 °C and 5% CO_2. After extensive washing, the 12-well plate was moved upon the stage of a Confocal Microscope Leica SP8 equipped with an Okolab stage-top incubator for live cell imaging at 37 °C and 5% CO_2 and a Leica HC PL Fluotar objective 20x objective (6.9 mm working distance, 0.4 numerical aperture). The experiments were performed at the Confocal Microscopy Facility of the Centro Grandi Strumenti, University of Pavia.

Immunoblotting

Total protein homogenates from primary mCRC cells were treated with a RIPA buffer containing (150 mM NaCl, 0.5% sodium deoxycholate, 0.1% SDS, 0.1% Triton X-100, 50 mM Tris-HCl, pH 8, and the protease inhibitor cocktail cOmplete (cOmplete Tablets EASYpack, 04693116001; Merck, Milan, Italy). Laemmli buffer was added to the samples, and denaturation was made by heating in a thermal block for 10 min at 80 °C. Twenty µicrograms of proteins were loaded in precast polyacrylamide gel (4–20% Mini-PROTEAN TGX Stain-Free Gels, Bio-Rad, Segrate, Italy) and SDS-PAGE performed [57]. Then, the proteins were transferred out of the gel onto the PVDF Membrane (Trans-Blot Turbo Transfer Pack, #1704156, Bio-Rad, Segrate, Italy) with the Trans-Blot Turbo Transfer apparatus (#1704150, Bio-Rad, Segrate, Italy). Membranes were blocked by incubation for 1 h at 22 °C in Tris-buffered saline with 5% skimmed dry milk and 0.1% Tween (blocking solution). Membranes were incubated overnight with anti-TRPA1 rabbit antibody (PA146159, 1:500 dilution; Thermo Fisher Scientific, Monza, Italy) in the blocking solution. The membranes were washed three times and incubated for 1 h with goat anti-rabbit IgG antibody, peroxidase-conjugated (1:100000; AP132P; Millipore part of Merck S.p.a., Vimodrone, Italy). The detection of the bands was performed with the chemiluminescent substrate kit Westar Supernova Western (CYANAGEN, Bologna, Italy) and the molecular weights of the bands were pinpointed using pre-stained molecular weight markers (#161-0376, Bio-Rad Laboratories, California, USA). Stripped membranes were re-probed by incubating with the housekeeping anti-β-actin rabbit monoclonal antibody (AB-81599, 1: 2000; Immunological Sciences, Rome, Italy) [58]. Protein bands were visualized using the iBright™ CL1000 Imaging System (Thermo Fisher Scientific, Monza, Italy). The band intensity was semi-quantified by using iBright Analysis Software (Thermo Fisher Scientific, Monza, Italy) and the results were expressed as TRPA1 / β-actin ratio.

Gene silencing

Gene silencing of TRPA1 has been performed by using the same strategy as that employed to down-regulate the expression of STIM1 and Orai1 [40], TRP Vanilloid 1 [14] and two-pore channel 1 [13] in primary cultures of mCRC cells. The esiRNA targeting TRPA1 was purchased from Sigma-Aldrich Inc. MISSION®esiRNA (human TRPA1) (EHU040601). Negative controls were made by using scrambled siRNA. In brief, when mCRC cells reached 50% confluency, the medium was replaced with reduced serum medium Opti-MEM, (Life Technologies, Milan, Italy). The solution of siRNAs diluted (100 nM final concentration) with Opti-MEM was combined with Opti-MEM containing the Lipofectamine™ transfection reagent (Life Technologies, Milan, Italy), following the manufacturer's instructions. This solution containing siRNA was incubated for 20 min at room temperature. Finally, the siRNA-Lipofectamin complex was added to the cells and the cells were then left in a CO_2 incubator for 5 h. The siRNA-Lipofectamin complex was then eliminated, and fresh culture media was added to the cells. Protein silencing was effective 48 h after transfection. To check the knockdown efficiency, immunoblot for TRPA1 was performed in siRNA and Mock treated cells (see Figs. S3 and S4).

Statistics

All the data have been generated by mCRC and non-neoplastic cells expanded from three distinct patients. Each experiment has been carried out three times by using cells obtained by each patient in three separate days. The amplitude of cytosolic and mitochondrial Ca^{2+} signals evoked by each agonist (AITC, H_2O_2, and 4-HNE) was measured as the difference between the F_{340}/F_{380} ratio at the peak of the Ca^{2+} signal and the mean F_{340}/F_{380} ratio of 1 min baseline recorded before addition of the agonist. The dose-response relationship reported in Fig. S5B was fitted by using the equation [59]:

$$Y = \frac{100}{1 + \frac{EC_{50}}{[H202]}} \quad (1)$$

where Y is the amplitude of the Ca^{2+} response, $[H_2O_2]$ is the H_2O_2 concentration, and EC_{50} is the half-maximal effective concentration.

Pooled data are presented as mean ± SE. The number of cells analyzed for each condition is indicated in the corresponding bar histograms. Normality of the data was tested with Shapiro–Wilk test. If the data distribution was normal, differences between two groups were evaluated by using the Student's *t*-test for unpaired observations, whereas Differences between multiple groups were evaluated by using one-way ANOVA analysis followed by the post hoc Dunnett's or Bonferroni tests as appropriate. $p < 0.05$ indicated statistical significance. No statistical methods were used to predetermine the sample size.

Chemicals

Fura-2/AM and Rhod-2/AM were purchased from Invitrogen (Life Technologies). All the chemicals were purchased from Sigma-Aldrich .

DATA AVAILABILITY

All the data generated or analyzed in this study are available upon reasonable request to the corresponding authors.

REFERENCES

1. Lichtenstern CR, Ngu RK, Shalapour S, Karin M. Immunotherapy, Inflammation and Colorectal. Cancer Cells. 2020;9:3.
2. Gorrini C, Harris IS, Mak TW. Modulation of oxidative stress as an anticancer strategy. Nat Rev Drug Discov. 2013;12:931–47.
3. Basak D, Uddin MN, Hancock J. The role of oxidative stress and its counteractive utility in colorectal cancer (CRC). Cancers (Basel). 2020;12:11.
4. Tasdogan A, Ubellacker JM, Morrison SJ. Redox regulation in cancer cells during metastasis. Cancer Discov. 2021;11:2682–92.
5. Conklin KA. Chemotherapy-associated oxidative stress: impact on chemotherapeutic effectiveness. Integr Cancer Ther. 2004;3:294–300.

6. Talavera K, Startek JB, Alvarez-Collazo J, Boonen B, Alpizar YA, Sanchez A, et al. Mammalian transient receptor potential TRPA1 channels: from structure to disease. Physiol Rev. 2020;100:725–803.
7. Sakaguchi R, Mori Y. Transient receptor potential (TRP) channels: Biosensors for redox environmental stimuli and cellular status. Free Radic Biol Med. 2020;146:36–44.
8. Reczek CR, Chandel NS. ROS promotes cancer cell survival through calcium signaling. Cancer Cell. 2018;33:949–51.
9. Takahashi N, Chen HY, Harris IS, Stover DG, Selfors LM, Bronson RT, et al. Cancer cells co-opt the neuronal redox-sensing channel TRPA1 to promote oxidative-stress tolerance. Cancer Cell. 2018;33:985–1003.e7.
10. Deveci HA, Akyuva Y, Nur G, Naziroglu M. Alpha lipoic acid attenuates hypoxia-induced apoptosis, inflammation and mitochondrial oxidative stress via inhibition of TRPA1 channel in human glioblastoma cell line. Biomed Pharmacother. 2019;111:292–304.
11. Chen H, Li C, Hu H, Zhang B. Activated TRPA1 plays a therapeutic role in TMZ resistance in glioblastoma by altering mitochondrial dynamics. BMC Mol Cell Biol. 2022;23:38.
12. Kiss F, Kormos V, Szoke E, Kecskes A, Toth N, Steib A, et al. Functional transient receptor potential ankyrin 1 and vanilloid 1 ion channels are overexpressed in human oral squamous cell carcinoma. Int J Mol Sci. 2022;23:3.
13. Faris P, Pellavio G, Ferulli F, Di Nezza F, Shekha M, Lim D, et al. Nicotinic acid adenine dinucleotide phosphate (NAADP) induces intracellular Ca(2+) release through the two-pore channel TPC1 in metastatic colorectal cancer Cells. Cancers (Basel). 2019;11:pii: E542.
14. Faris P, Ferulli F, Vismara M, Tanzi M, Negri S, Rumolo A, et al. Hydrogen sulfide-evoked intracellular Ca(2+) signals in primary cultures of metastatic colorectal cancer cells. Cancers (Basel). 2020;12:11.
15. Faris P, Rumolo A, Tapella L, Tanzi M, Metallo A, Conca F, et al. Store-operated Ca(2+) entry is up-regulated in tumour-infiltrating lymphocytes from metastatic colorectal cancer patients. Cancers (Basel). 2022;14:14.
16. Fliniaux I, Germain E, Farfariello V, Prevarskaya N. TRPs and Ca(2+) in cell death and survival. Cell Calcium. 2018;69:4–18.
17. Moccia F, Dragoni S, Poletto V, Rosti V, Tanzi F, Ganini C, et al. Orai1 and transient receptor potential channels as novel molecular targets to impair tumor neovascularisation in renal cell carcinoma and other malignancies. Anticancer Agents Med Chem. 2014;14:296–12.
18. Li L, Chen C, Chiang C, Xiao T, Chen Y, Zhao Y, et al. The impact of TRPV1 on cancer pathogenesis and therapy: a systematic review. Int J Biol Sci. 2021;17:2034–49.
19. Ibrahim S, Dakik H, Vandier C, Chautard R, Paintaud G, Mazurier F, et al. Expression profiling of calcium channels and calcium-activated potassium channels in colorectal cancer. Cancers (Basel). 2019;11:4.
20. Cojocaru F, Selescu T, Domocos D, Marutescu L, Chiritoiu G, Chelaru NR, et al. Functional expression of the transient receptor potential ankyrin type 1 channel in pancreatic adenocarcinoma cells. Sci Rep. 2021;11:2018.
21. Derouiche S, Mariot P, Warnier M, Vancauwenberghe E, Bidaux G, Gosset P, et al. Activation of TRPA1 channel by antibacterial agent triclosan induces VEGF secretion in human prostate cancer stromal cells. Cancer Prev Res (Philos). 2017;10:177–87.
22. Dragoni S, Turin I, Laforenza U, Potenza DM, Bottino C, Glasnov TN, et al. Store-operated Ca2+ entry does not control proliferation in primary cultures of human metastatic renal cellular carcinoma. BioMed Res Int. 2014;2014:739494.
23. Kusiak AA, Jakubowska MA, Stopa KB, Zhang X, Huang W, Gerasimenko JV, et al. Activation of pancreatic stellate cells attenuates intracellular Ca(2+) signals due to downregulation of TRPA1 and protects against cell death induced by alcohol metabolites. Cell Death Dis. 2022;13:744.
24. Chen YF, Chiu WT, Chen YT, Lin PY, Huang HJ, Chou CY, et al. Calcium store sensor stromal-interaction molecule 1-dependent signaling plays an important role in cervical cancer growth, migration, and angiogenesis. Proc Natl Acad Sci USA. 2011;108:15225–30.
25. Doskey CM, Buranasudja V, Wagner BA, Wilkes JG, Du J, Cullen JJ, et al. Tumor cells have decreased ability to metabolize H(2)O(2): Implications for pharmacological ascorbate in cancer therapy. Redox Biol. 2016;10:274–84.
26. Negri S, Faris P, Tullii G, Vismara M, Pellegata AF, Lodola F, et al. Conjugated polymers mediate intracellular Ca(2+) signals in circulating endothelial colony forming cells through the reactive oxygen species-dependent activation of Transient Receptor Potential Vanilloid 1 (TRPV1). Cell Calcium. 2022;101:102502.
27. DelloStritto DJ, Connell PJ, Dick GM, Fancher IS, Klarich B, Fahmy JN, et al. Differential regulation of TRPV1 channels by H_2O_2: implications for diabetic microvascular dysfunction. Basic Res Cardiol. 2016;111:21.
28. Martinotti S, Laforenza U, Patrone M, Moccia F, Ranzato E. Honey-mediated wound healing: H(2)O(2) entry through AQP3 determines extracellular Ca(2+) influx. Int J Mol Sci. 2019;20:3.
29. De Logu F, Souza Monteiro de Araujo D, Ugolini F, Iannone LF, Vannucchi M, Portelli F, et al. The TRPA1 channel amplifies the oxidative stress signal in melanoma. Cells. 2021;10:11.
30. Oehler B, Kloka J, Mohammadi M, Ben-Kraiem A, Rittner HL. D-4F, an ApoA-I mimetic peptide ameliorating TRPA1-mediated nocifensive behaviour in a model of neurogenic inflammation. Mol Pain. 2020;16:1744806920903848.
31. Sullivan MN, Gonzales AL, Pires PW, Bruhl A, Leo MD, Li W, et al. Localized TRPA1 channel Ca2+ signals stimulated by reactive oxygen species promote cerebral artery dilation. Sci Signal. 2015;8:ra2.
32. Kerkhofs M, La Rovere R, Welkenhuysen K, Janssens A, Vandenberghe P, Madesh M, et al. BIRD-2, a BH4-domain-targeting peptide of Bcl-2, provokes Bax/Bak-independent cell death in B-cell cancers through mitochondrial Ca(2+)-dependent mPTP opening. Cell Calcium. 2021;94:102333.
33. Giorgi C, Baldassari F, Bononi A, Bonora M, De Marchi E, Marchi S, et al. Mitochondrial Ca(2+) and apoptosis. Cell Calcium. 2012;52:36–43.
34. Shen L, Wen N, Xia M, Zhang YU, Liu W, Xu YE, et al. Calcium efflux from the endoplasmic reticulum regulates cisplatin-induced apoptosis in human cervical cancer HeLa cells. Oncol Lett. 2016;11:2411–9.
35. Pathak T, Gueguinou M, Walter V, Delierneux C, Johnson MT, Zhang X, et al. Dichotomous role of the human mitochondrial Na(+)/Ca2(+)/Li(+) exchanger NCLX in colorectal cancer growth and metastasis. eLife. 2020;9:e59686.
36. McMahon DB, Kuek LE, Johnson ME, Johnson PO, Horn RLJ, Carey RM, et al. The bitter end: T2R bitter receptor agonists elevate nuclear calcium and induce apoptosis in non-ciliated airway epithelial cells. Cell Calcium. 2022;101:102499.
37. Oroz-Parra I, Navarro M, Cervantes-Luevano KE, Alvarez-Delgado C, Salvesen G, Sanchez-Campos LN, et al. Apoptosis activation in human lung cancer cell lines by a novel synthetic peptide derived from conus californicus venom. Toxins (Basel). 2016;8:38.
38. Zhou H, Liu Z, Wang Y, Wen X, Amador EH, Yuan L, et al. Colorectal liver metastasis: molecular mechanism and interventional therapy. Signal Transduct Target Ther. 2022;7:70.
39. Turin I, Schiavo R, Maestri M, Luinetti O, Dal Bello B, Paulli M, et al. In vitro efficient expansion of tumor cells deriving from different types of human tumor samples. Med Sci. 2014;2:70–81.
40. Zuccolo E, Laforenza U, Ferulli F, Pellavio G, Scarpellino G, Tanzi M, et al. Stim and Orai mediate constitutive Ca(2+) entry and control endoplasmic reticulum Ca(2+) refilling in primary cultures of colorectal carcinoma cells. Oncotarget. 2018;9:31098–19.
41. Rosa N, Ivanova H, Wagner LE II, Kale J, La Rovere R, Welkenhuyzen K, et al. Bcl-xL acts as an inhibitor of IP(3)R channels, thereby antagonizing Ca(2+)-driven apoptosis. Cell Death Differ. 2022;29:788–805.
42. Hausmann D, Hoffmann DC, Venkataramani V, Jung E, Horschitz S, Tetzlaff SK, et al. Autonomous rhythmic activity in glioma networks drives brain tumour growth. Nature. 2023;613:179–86.
43. Astesana V, Faris P, Ferrari B, Siciliani S, Lim D, Biggiogera M, et al. [Pt(O,O'-acac)(gamma-acac)(DMS)]: alternative strategies to overcome cisplatin-induced side effects and resistance in T98G glioma cells. Cell Mol Neurobiol. 2020;41:563–87.
44. Zhong H, Yin H. Role of lipid peroxidation derived 4-hydroxynonenal (4-HNE) in cancer: focusing on mitochondria. Redox Biol. 2015;4:193–9.
45. Negri S, Faris P, Moccia F. Reactive oxygen species and endothelial Ca(2+) signaling: brothers in arms or partners in crime? Int J Mol Sci. 2021;22:9821.
46. Andersson DA, Gentry C, Moss S, Bevan S. Transient receptor potential A1 is a sensory receptor for multiple products of oxidative stress. J Neurosci. 2008;28:2485–94.
47. Yin S, Zhang L, Ding L, Huang Z, Xu B, Li X, et al. Transient receptor potential ankyrin 1 (trpa1) mediates il-1beta-induced apoptosis in rat chondrocytes via calcium overload and mitochondrial dysfunction. J Inflamm (Lond). 2018;15:27.
48. Tian C, Han X, He L, Tang F, Huang R, Lin Z, et al. Transient receptor potential ankyrin 1 contributes to the ATP-elicited oxidative stress and inflammation in THP-1-derived macrophage. Mol Cell Biochem. 2020;473:179–92.
49. Loncke J, Kaasik A, Bezprozvanny I, Parys JB, Kerkhofs M, Bultynck G. Balancing ER-mitochondrial Ca(2+) fluxes in health and disease. Trends Cell Biol. 2021;31:598–12.
50. Giorgi C, Romagnoli A, Pinton P, Rizzuto R. Ca2+ signaling, mitochondria and cell death. Curr Mol Med. 2008;8:119–30.
51. Ozkal B, Ovey IS. Selenium enhances TRPA1 channel-mediated activity of temozolomide in SH-SY5Y neuroblastoma cells. Childs Nerv Syst. 2020;36:1283–92.
52. Souza Monteiro de Araujo D, De Logu F, Adembri C, Rizzo S, Janal MN, Landini L, et al. TRPA1 mediates damage of the retina induced by ischemia and reperfusion in mice. Cell Death Dis. 2020;11:633.
53. Lu F, Sun J, Zheng Q, Li J, Hu Y, Yu P, et al. Imaging elemental events of store-operated Ca(2+) entry in invading cancer cells with plasmalemmal targeted sensors. J Cell Sci. 2019;132:6.
54. Vismara M, Negri S, Scolari F, Brunetti V, Trivigno SMG, Faris P, et al. Platelet-derived extracellular vesicles stimulate migration through partial remodelling of the Ca(2+) handling machinery in MDA-MB-231 breast cancer cells. Cells. 2022;11:19.
55. Alharbi A, Zhang Y, Parrington J. Deciphering the role of Ca(2+) signalling in cancer metastasis: from the bench to the bedside. Cancers (Basel). 2021;13:2.
56. Balducci V, Faris P, Balbi C, Costa A, Negri S, Rosti V, et al. The human amniotic fluid stem cell secretome triggers intracellular Ca(2+) oscillations, NF-kappaB

nuclear translocation and tube formation in human endothelial colony-forming cells. J Cell Mol Med. 2021;25:8074–86.
57. Laemmli UK. Cleavage of structural proteins during the assembly of the head of bacteriophage T4. Nature. 1970;227:680–5.
58. Yeung YG, Stanley ER. A solution for stripping antibodies from polyvinylidene fluoride immunoblots for multiple reprobing. Anal Biochem. 2009;389:89–91.
59. Berra-Romani R, Faris P, Pellavio G, Orgiu M, Negri S, Forcaia G, et al. Histamine induces intracellular Ca(2+) oscillations and nitric oxide release in endothelial cells from brain microvascular circulation. J Cell Physiol. 2020;235:1515–30.

ACKNOWLEDGEMENTS

We truly thank Dr. Amanda Oldani for her valuable technical support to measure the kinetics of TRPA1-induced caspase-3/7 activation with the Confocal Microscope Leica SP8 at the Confocal Microscopy Facility of the Centro Grandi Strumenti, University of Pavia.

AUTHOR CONTRIBUTIONS

DM and FM performed study concept and design; DM and FM performed development of methodology and writing, review and revision of the paper; PF, AR, GP, MT, MV, and AG provided acquisition, analysis and interpretation of data, and statistical analysis; SC, PP, and UL provided technical and material support. All authors read and approved the final manuscript.

FUNDING

This research was funded by: Fondo Ricerca Giovani from the University of Pavia (FM), Italian Ministry of Education, University and Research (MIUR): Dipartimenti di Eccellenza Program (2018–2022)—Dept. of Biology and Biotechnology "L. Spallanzani", University of Pavia (FM), Program "Ricerca Corrente 08059819" of the Foundation IRCCS Policlinico San Matteo, Pavia (DM).

COMPETING INTERESTS

The authors declare no competing interests.

ETHICS APPROVAL AND CONSENT TO PARTICIPATE

The Foundation IRCCS Policlinico San Matteo approved the present study (Ethical code 20110000996, 17/01/2011).

ADDITIONAL INFORMATION

Supplementary information The online version contains supplementary material available at https://doi.org/10.1038/s41420-023-01530-x.

Correspondence and requests for materials should be addressed to Daniela Montagna or Francesco Moccia.

Reprints and permission information is available at http://www.nature.com/reprints

Publisher's note Springer Nature remains neutral with regard to jurisdictional claims in published maps and institutional affiliations.